CrossMark

The NEO Surveyor Near-Earth Asteroid Known Object Model

Tommy Grav[1] , Amy K. Mainzer[1] , Joseph R. Masiero[2] , Dar W. Dahlen[2] , Tim Spahr[3], William F. Bottke[4] , and Frank J. Masci[2]

[1] University of Arizona, Lunar and Planetary Laboratory, 1629 E. University Boulevard, Tucson, AZ 85721-0092, USA; tgrav@arizona.edu
[2] IPAC, California Institute of Technology, 1200 E. California Boulevard, Pasadena, CA 91125, USA
[3] NEO Sciences, USA
[4] Southwest Research Institute, Solar System Science and Exploration Division, 1050 Walnut Street, Suite 300, Boulder, CO 80302, USA

Abstract

The known near-Earth object (NEO) population consists of over 32,000 objects, with a yearly discovery rate of over 3000 NEOs per year. An essential component of the next generation of NEO surveys is an understanding of the population of known objects, including an accounting of the discovery rate per year as a function of size. Using a near-Earth asteroid (NEA) reference model developed for NASA's NEO Surveyor (NEOS) mission and a model of the major current and historical ground-based surveys, an estimate of the current NEA survey completeness as a function of size and absolute magnitude has been determined (termed the Known Object Model; KOM). This allows for understanding of the intersection of the known catalog of NEAs and the objects expected to be observed by NEOS. The current NEA population is found to be ~38% complete for objects larger than 140 m, consistent with estimates by Harris & Chodas. NEOS is expected to catalog more than two-thirds of the NEAs larger than 140 m, resulting in ~76% of NEAs cataloged at the end of its 5 yr nominal survey, making significant progress toward the US Congressional mandate. The KOM estimates that ~77% of the currently cataloged objects will be detected by NEOS, with those not detected contributing ~9% to the final completeness at the end of its 5 yr mission. This model allows for placing the NEOS mission in the context of current surveys to more completely assess the progress toward the goal of cataloging the population of hazardous asteroids.

1. Introduction

The near-Earth object (NEO) population is made up of asteroids and comets that are on orbits that take them close to Earth. NEOs are defined as objects with orbits that bring them closer than 1.3 au (perihelion distance $q \leqslant 1.3$ au) from the Sun. They consist of both active and nonactive bodies, where the near-Earth comets make up about 5%–15% of the NEO population (Wetherill 1987, 1988; Bottke et al. 2002; Bauer et al. 2017; Granvik et al. 2018). In this paper, we will focus on the near-Earth asteroid (NEA) population exclusively.

The NEAs can be split into four main subpopulations. The largest of these subpopulations is the Apollos, named after one of its members, (1862) Apollo. They are defined as objects with semimajor axis $a > 1$. au and perihelion distance $q \leqslant 1.017$ au, consisting mainly of objects whose orbits cross the orbit of the Earth. The Amors, named after their archetype object (1221) Amor, are defined as objects with perihelion distance 1.017 au $< q \leqslant 1.3$ au. The Amors are the second-largest group, consisting of objects whose orbits are entirely outside the Earth's orbit. The Atens are defined as objects with semimajor axis $a < 1$ au and aphelion distance $Q > 0.983$ au. They consist of objects with orbits that are mainly inside the orbit of the Earth but cross the orbit of the Earth. The smallest of the four subpopulations is the Atiras, named after the first known object of its kind, (163693) Atira. These objects have orbits with aphelion $Q \leqslant 0.983$ au, putting their entire orbit inside the Earth's orbit. Figure 1 shows the four subpopulations in the semimajor axis and eccentricity space.

The Minor Planet Center (MPC)[5] maintains the official catalog of observations and orbital elements for asteroids, comets, and natural satellites in our solar system. At the beginning of 2023 June, the MPC Catalog contained orbits and observations of more than 32,100 NEAs, of which about a quarter are potentially hazardous asteroids (PHAs), which have a minimum orbital intersection distance (MOID) of $\leqslant 0.05$ au. Usually the definition of PHAs includes a selection criterion of $H_V \leqslant 22$ mag, with this being traditionally used as a proxy for a diameter of $\geqslant 140$ m. However, in this work, we consider any object with MOID $\leqslant 0.05$ au to be a PHA, as a dark object with a diameter of 140 m can have an absolute magnitude as faint as $H_V \sim 24$ mag.

The Apollos make up ~51.2% of this cataloged data set; ~40.8% of the cataloged NEAs are Amors, and ~7.8% are Atens. Less than 0.2% of the known NEAs are Atiras. Figure 2 shows that the cumulative fractions are relatively stable up to about absolute magnitude $H_V \sim 20$ mag, but for higher absolute magnitudes, the fraction of NEAs that are Atens starts rising slightly. The relative fraction of Amors and Apollos remains stable until $H_V \sim 24$ mag; at higher absolute magnitude values, the fraction of Apollos starts rising significantly. These fractions are influenced by observational biases, especially at smaller sizes (higher absolute magnitudes), due to the observational geometry. A closer look at these observational biases will be discussed in Section 4.

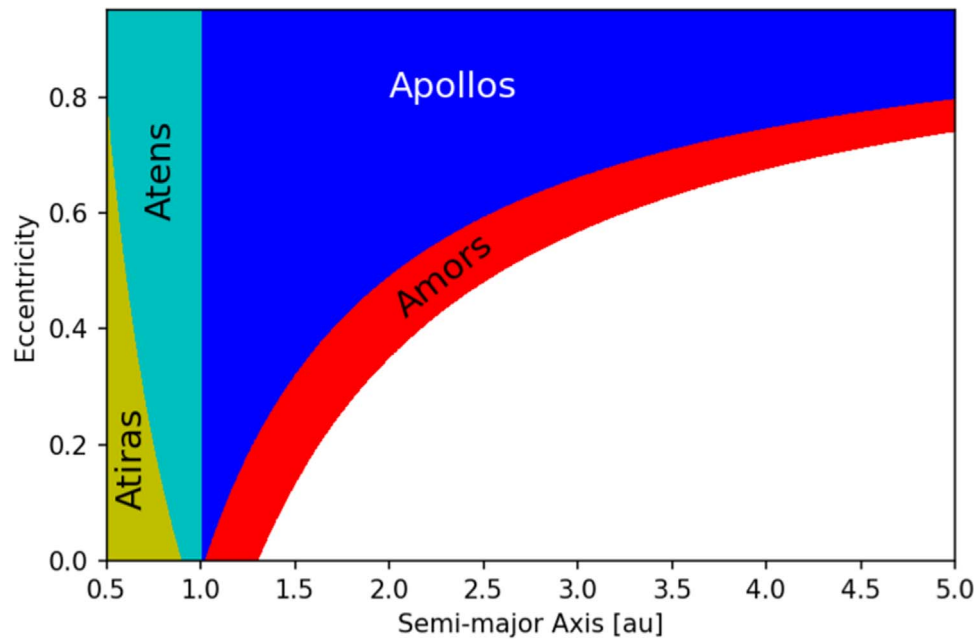---

[5] https://minorplanetcenter.net

Figure 1. A schematic showing the region in semimajor axis vs. eccentricity space of the four NEO subpopulations.
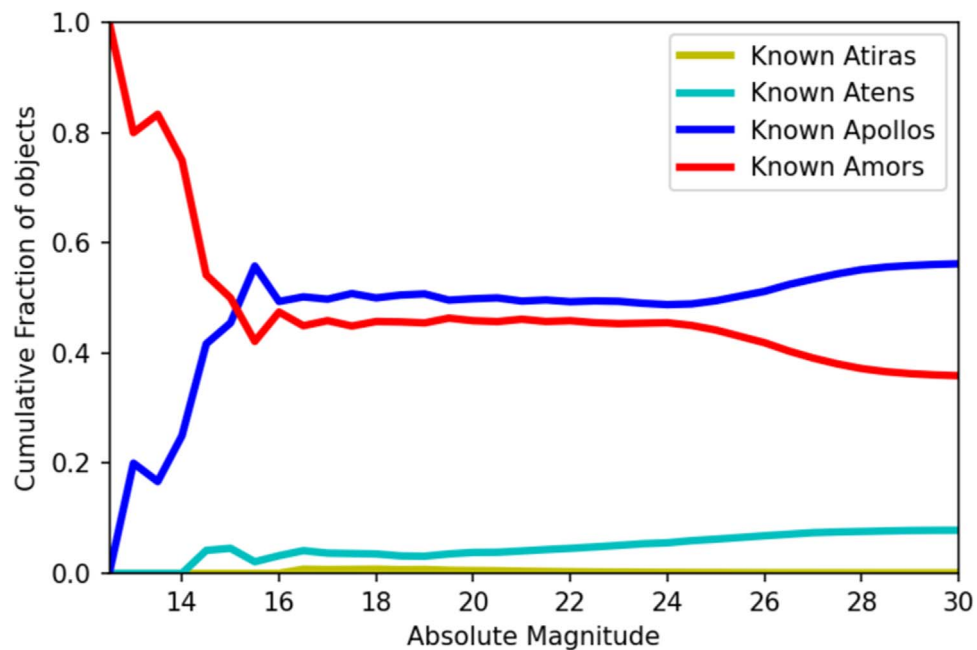

Figure 2. The fraction of each NEA subpopulation (Atiras, Atens, Apollos, and Amors) from the MPC catalog as a function of absolute magnitude. The fractions for a value of absolute magnitude are cumulative, including all objects with values less than the value plotted. The effects of observational bias are clearly seen at $H_V > 24$ mag.

In studies of NEAs, two diameter regimes have become important: the objects thought to be larger than 1 km and the population between 140 m and 1 km. The largest objects, with effective diameters larger than 1 km, impact infrequently. But these objects possess the power to cause global extinction events (Alvarez et al. 1980). It is estimated that these objects pose about 90% of the risk from asteroid impacts, and the "Spaceguard" (Milani et al. 1990; Morrison 1992) goal of discovering 90% of asteroids in this size range was created to address this risk. This goal was found to have been completed around 2010 (Mainzer et al. 2011a; Granvik et al. 2018). Community studies (Stokes et al. 2003, 2017; National

Academies of Sciences, Engineering, and Medicine 2019) have found that after the Spaceguard goal was achieved, the majority of the remaining risk lay with asteroids larger than 140 m, which are capable of creating significant local or regional damage upon impact. The George E. Brown, Jr. Near-Earth Object Survey Act was passed by the United States Congress in 2005, directing that NASA by 2020 detect and track more than 90% of all NEOs larger than 140 m in effective diameter.[6] New discoveries have been dominated by the Catalina Sky Survey (CSS; MPC observatory codes 703 and G96) and Pan-

_____
[6] https://www.congress.gov/bill/109th-congress/house-bill/1022/text

STARRS (PS; MPC observatory codes F51 and F52) over the last decade, together accounting for 80%–92% of discoveries every year covering that time period. In Section 2.1, we will take a closer look at the discovery statistics over the last decade and their implications for understanding the current completeness level of the known NEA population.

One of the fundamental problems in the field of planetary defense is that the goals outlined by Spaceguard and the George E. Brown, Jr. Act are defined in diameter, since impact energy depends on diameter to the third power ($\sim D^3$); therefore, accurate knowledge of diameter is important for constraining impact energy. The current major surveys obtain observations at visible wavelengths, allowing for the derivation of orbital parameters and absolute magnitude, but these bandpasses do not allow for direct derivation of the effective spherical diameter. The absolute magnitude at visible wavelengths, H_V, is defined as the theoretical visible magnitude an object would have if it was 1 au from the Sun and Earth at zero phase angle. If the reflectivity of the object is known, i.e., the visible geometric albedo, the size of the object can be determined by $D = (1329/\sqrt{p_V}) * 10^{-0.2H}$ (Tedesco et al. 1992), where D is the diameter in kilometers, p_V is the geometric albedo at visible wavelengths, and H_V is the absolute magnitude. Traditionally, an albedo of $p_V = 0.14$ has been assumed, which yields $H_V = 22$ mag for an object with a diameter of 140 m and $H_V = 17.75$ mag for an object with a 1 km diameter. However, infrared missions like IRAS (Tedesco et al. 1992, 2002), NEOWISE (Mainzer et al. 2011a, 2011b; Wright et al. 2016), and Akari (Usui et al. 2011) showed that the geometric albedo for asteroids varies from about 2% to 60%, with the dark component of the population having a Maxwellian distribution peaking at $\sim$3% and the rest in a Maxwellian distribution peaking at $\sim$17% (Wright et al. 2016). About 40% of the NEOs of a given size have $p_V < 0.1$ (Mainzer et al. 2011c). This introduces complexity in understanding the completeness for effective diameter-limited samples when a majority of observations are obtained at visible wavelengths. Wright et al. (2016) examined what equivalent H_V magnitude would be required in order to reach 90% completeness for NEAs larger than 140 m considering the double Maxwellian distribution of the NEA albedo distribution derived by the NEOWISE mission. They found that in order to reach 90% survey completeness for this size range, a 90% completeness of objects with $H_V \leqslant 23$ mag is needed. We thus use $H_V \leqslant 23$ mag as the appropriate proxy for objects larger than 140 m in this paper, rather than the traditional $H_V = 22$ mag.

In this paper, we examine the known population of NEAs and how this population will be observed by the NEO Surveyor (NEOS) mission (Mainzer et al. 2023) and compliment its expected performance. NEOS is part of the next-generation surveys for asteroids that could impact the Earth. Previously known as NEOCam (Mainzer et al. 2015), NEOS is a space mission designed to detect, track, and characterize NEAs using thermal emission observations. It recently passed NASA's preliminary design review phase and is scheduled to launch in 2027 September. It is designed to catalog more than two-thirds of the PHAs larger than 140 m in diameter by the end of its nominal 5 yr mission. NEOS uses a reference model of synthetic asteroids and comets to gauge its performance and progress against this goal. See Mainzer et al. (2023) for additional information on the NEOS reference model.

However, since the catalog of NEAs and PHAs is not empty at the time of the start of the NEOS mission, it is important to determine a set of proxy objects in the synthetic reference model that represents the currently known objects. This allows for understanding of what types of objects among the current MPC catalog are unlikely to be detected by NEOS and thus would count toward the cataloging goal and which objects that are currently known are likely to also be detected by NEOS, providing both optical and thermal observations that allow for determination of both diameter and geometric albedo. While future ground-based surveys, such as the Vera Rubin Observatory (Vereš & Chesley 2017; Jones et al. 2018), will also contribute to the total number of cataloged NEOs, the actual performance of these future surveys is still in the planning phases, which could potentially have large impacts on their performance in terms of NEO discovery. A study of the performance of the Vera Rubin Observatory (then the Large Synoptic Sky Telescope) and its synergy and overlap with NEOS (then the NEOCam mission) can be found in Grav et al. (2016). Thus, this paper provides a worst-case scenario, where no additional future NEAs are assumed to have been discovered prior to the NEOS launch.

We note that this paper uses data from the MPC catalog extracted on 2023 September 5. The orbits and absolute magnitudes of objects cataloged by the MPC are in a constant state of flux, as additional observations are continuously being submitted by observers from around the world. In this paper, we compare our results to those of Harris & Chodas (2021), but we note here that recent recalculations in the absolute magnitudes for NEOs cataloged has yielded a revision in the number of large NEOs (A. W. Harris, 2023, personal communications).[7] The revision resulted in a change of $\sim$100 fewer NEOs with $H_V < 17.75$ mag compared to the data used in Harris & Chodas (2021), meaning that the NEOs were, on average, revised to 0.13 mag fainter. This is in line with Pravec et al. (2012), comparing the absolute magnitudes from the MPC catalog with a list of asteroids with high-precision photometric observations, which found that the absolute magnitudes in the MPC catalog were, on average, 0.3 mag too bright.

We examine the current status of the NEA and PHA populations cataloged by the MPC (Section 2). In Section 3, we discuss the NEOS mission, along with the NEOS Survey Simulator (NSS) and the NEOS reference model, two tools used to predict the performance of the NEOS mission in detecting, tracking, and characterizing small bodies in our solar system during its 5 yr nominal mission. The NEOS Known Object Model (KOM) is described in Section 4; this model is applied to the NEOS reference model to determine which of the synthetic objects would be expected to be present in the currently known population. Section 5 examines what portion of the known population is detected by the NEOS survey and which objects remain undetected at the end of the 5 yr nominal mission. Finally, Section 6 discusses the findings of this paper.

2. The Known NEA Population

At the beginning of 2023 June, the MPC catalog contained more than 32,100 NEAs. Of these, just over 3000 NEAs have been numbered, indicating that their orbits are well known and do not require additional observations to maintain accurate

---

positional predictions over the next century. An additional ~2000 NEAs have observations spanning more than 10 yr, with 10% of these spanning more than 20 yr, all of which should become numbered in the near future. Only a third of the known NEAs have multi-opposition orbits, with observations at two or more opposition epochs. A majority of the NEAs are only observed during their discovery apparitions, with almost half having been observed for less than 7 days, leaving them basically lost and in need of rediscovery to further refine their orbital parameters.

As mentioned above, the NEA population is divided into four subpopulations. However, the MPC catalog has a heavy observational bias toward certain of these subpopulations, especially the Atens and Apollos, as these objects tend to come much closer to the Earth and can thus be observed at much smaller sizes. Therefore, it is important to look at absolute magnitude–limited samples of the NEAs when considering fractions. When looking at the population of 853 objects with $H_V < 17.75$ mag, the fraction of objects in the subpopulations are 0.9%, 3.9%, 50.1%, and 45.1% for the Atiras, Atens, Apollos, and Amors, respectively. For the more than 13,000 NEAs with $H_V < 23$ mag, the proxy we are using for 140 m, the fractions have changed slightly to 0.2%, 5.1%, 49.2%, and 45.5% for the Atiras, Atens, Apollos, and Amors, respectively.

Figure 2 shows the fractions for the four subpopulations when including all objects with a certain absolute magnitude range. The fractions stay relatively consistent to about $H_V \sim 24$ mag, where the observational effects favoring discovery of Apollos and Atens become apparent. There is an increase in the number of Atens from 3.9% at $H_V \leqslant 17.75$ mag to 5.1% at $H_V \leqslant 23$ mag, which comes at the expense of the Atira and Apollo subpopulations. This increase in numbers could be due to the effect of observational biases being more strongly apparent at smaller absolute magnitudes than those of the Apollos and Amors. Alternatively, the change could represent a real increase in Atens compared to other populations due to a difference in the source populations replenishing this subpopulation (Bottke et al. 2002). The relative fractions of objects discussed in this section are used when generating the NEOS reference model, which generates a synthetic population of NEAs by using physical parameter models derived using the NEOWISE mission for each subpopulation (Mainzer et al. 2012, 2023).

2.1. The Discovery Rate of NEOs

The number of discoveries of NEAs per year has sharply increased over the last few decades, from 27 discoveries in 1992, to 485 discoveries in 2002, to 991 discoveries a decade ago, to 3189 discoveries in 2022 (see Table 1 and Figures 3 and 4). These steady increases are due to the increases in effort and funding and improvement in technology, as touched upon in Section 1. While the total number of discoveries has sharply increased over the last decade, there has been a significant shift toward discovery of smaller objects. In 2012, objects with $H_V < 23$ mag made up almost 50% of all discoveries, but in 2022, that number declined to about 23% of discoveries for that year. This trend mirrors the trend seen in the largest objects ($H_V \leqslant 17.75$ mag), which constituted more than half of the discoveries in the mid-1980s. By the late 1990s, they only made up a quarter of the discoveries, even though the number of discovered objects had gone up dramatically (from ~tens of discoveries to more than 200 objects). Since then, the number

Table 1
The Yearly Discovery Statistics over the Last Decade

Year 23 ⩽ H	Total	H ⩽ 17.75		17.75 < H ⩽ 23			
2011	897	19	2.1%	477	53.2%	401	44.7%
2012	991	15	1.5%	480	48.4%	496	50.1%
2013	1029	11	1.1%	500	48.6%	518	50.3%
2014	1480	8	0.5%	651	44.0%	821	55.5%
2015	1551	7	0.5%	688	44.4%	856	55.2%
2016	1874	7	0.4%	731	39.0%	1136	60.6%
2017	2039	7	0.3%	743	36.4%	1289	63.2%
2018	1825	5	0.3%	614	33.6%	1206	66.1%
2019	2438	6	0.3%	750	30.8%	1682	69.0%
2020	2958	3	0.1%	829	28.0%	2126	71.9%
2021	3093	5	0.2%	730	23.6%	2358	76.2%
2022	3189	4	0.1%	725	22.7%	2460	77.1%

Note. Note that the H magnitude of all NEAs evolves as more observations are reported; thus, the reported numbers above might vary by a few objects when using a different MPC catalog instance than used here.

of discoveries per year of objects with $H_V \leqslant 17.75$ mag stayed at more than 45 objects for 8 yr before declining steadily year by year to the handful of objects discovered per year currently. This is due to the fact that the objects in this size regime are nearing observational completeness, with the remaining objects being increasingly difficult to discover due to their orbital geometry.

Currently, the number of yearly discoveries with $H_V \leqslant 23$ mag has stabilized at an average of 731 objects per year. Harris & Chodas (2021) found that there are between 31,341 objects with $H_V < 22.75$ mag and 47,577 objects with $H_V < 23.25$ mag, so we assume from this that there are ~39,500 objects with $H_V < 23$ mag. There are about 13,400 objects with $H_V \leqslant 23$ mag in the current MPC catalog, which means that to reach 90% completeness for $H_V \leqslant 23$ mag, as prescribed by Wright et al. (2016) in order to ensure 90% completeness for NEAs larger than 140 m, the current surveys would need to discover an additional 22,000 objects with $H_V \leqslant 23$ mag. At the current discovery rate, this would take more than 30 yr. As discussed for the objects with $H_V \leqslant 17.75$ mag, it is expected that the number of discoveries per year will decline as the completeness of the objects with $H_V \leqslant 23$ mag increases. This would significantly extend the time it would take for the current surveys to reach 90% survey completeness for NEAs with diameters larger than 140 m.

3. NEOS Mission

The NEOS is a NASA mission designed to find, catalog, and characterize NEAs. It is a single-instrument 50 cm space telescope operating in two infrared-wavelength channels, centered on 4.6 and 8 μm. At these wavelengths, thermal emission from NEAs dominates the observed flux due to their surface temperatures of 200–300 K. Situated at the Sun–Earth L1 Lagrange point, the mission will perform a nominal 5 yr survey, observing the field of regard of 45°–120° solar ecliptic longitude angle in the range of ±40° ecliptic latitude on either side of the Sun. Each of these sides takes about 6–7 days to complete, allowing NEOS to provide self-follow-up of its discoveries, as most of the moving objects will not have left the field of regard by the time the area is reobserved about 2 weeks later. NEOS is designed to catalog more than two-thirds of the
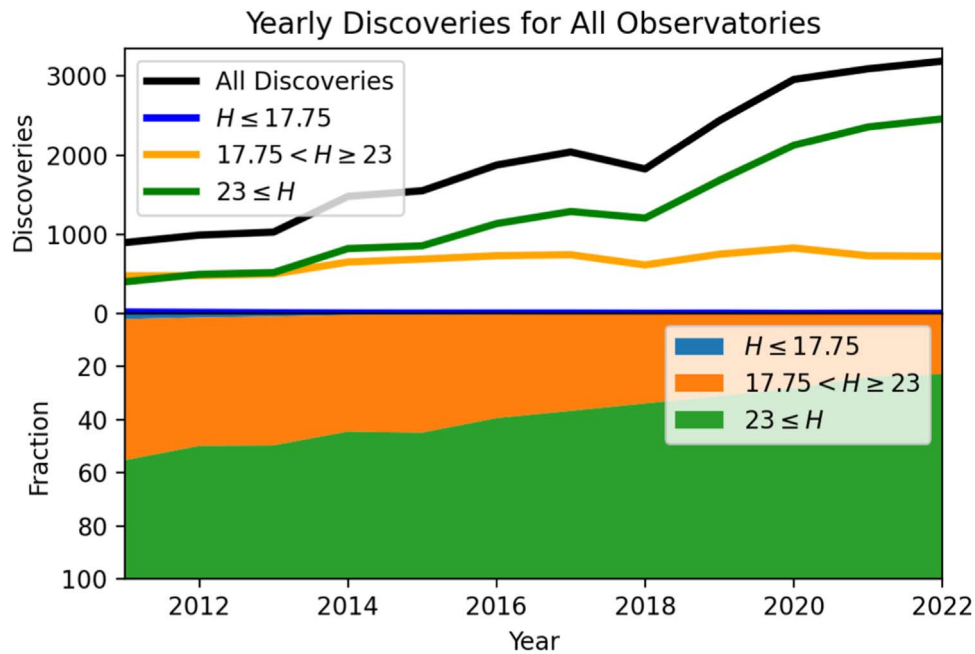
Figure 3. The discovery statistics over the last decade show that while the number of discoveries per year has risen regularly year over year, the fraction of objects with $H_V \leqslant 23$ mag has dropped by half from over half of the discoveries in 2011 to under a quarter of the discoveries in 2022.
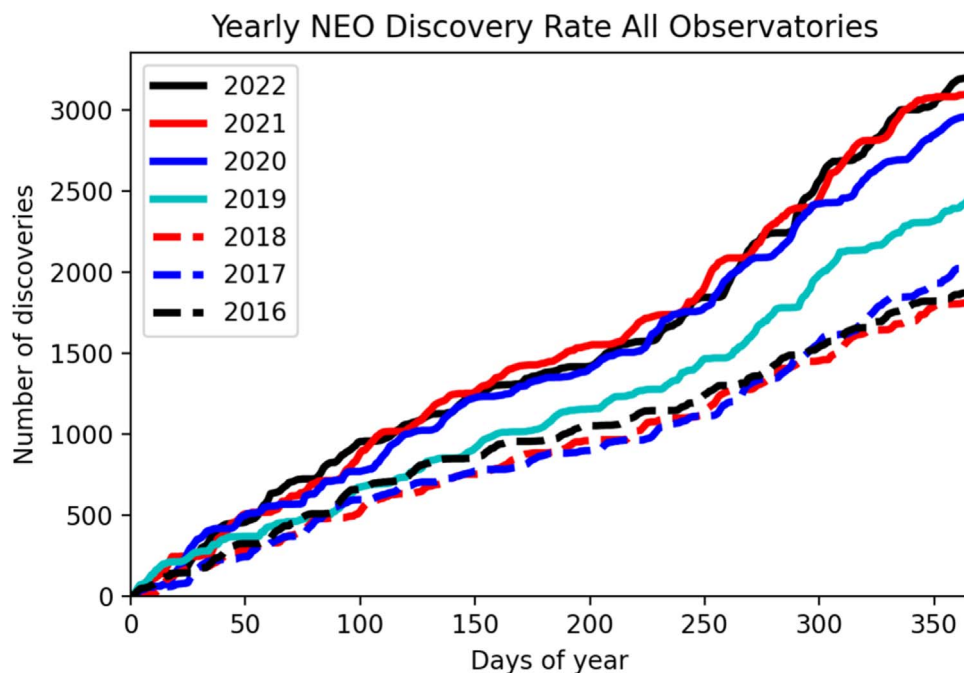

Figure 4. The yearly NEA discovery rate from 2016 to 2022.

PHAs larger than 140 m in diameter (Mainzer et al. 2023) by the end of its nominal 5 yr mission, with current models showing that it will reach more than 80% completeness for PHAs larger than 140 m. For a more in-depth description of NEOS and its mission, see Mainzer et al. (2023).

The NEOS project team has built a simulation tool, the NSS (Mainzer et al. 2015, 2023; Grav et al. 2016; Masiero et al. 2023), to understand the performance of the mission in making progress toward its design and the George E. Brown, Jr. goal. An integral part of evaluating the success of the NEOS mission is the use of the NEOS reference model, which contains a synthetic NEA population that the project uses as a "yardstick"

against which progress is measured. The NEA population of the reference model contains ~25,000 objects with diameters larger than 140 m. A kernel density estimator (Scott 1992; Virtanen et al. 2020) method using the NEA known population with $H_V < 20$ mag serves as the input for the orbital elements, and the NEOWISE data set (Mainzer et al. 2011b, 2012) is used as the basis for the model objects' physical properties (see Mainzer et al. 2023 for a more in-depth discussion of the NSS and the NEOS reference model). While the reference model is built using a size–frequency and albedo distribution based on the NEOWISE results, Figure 5 shows that the model is consistent with the absolute magnitude distribution found in the
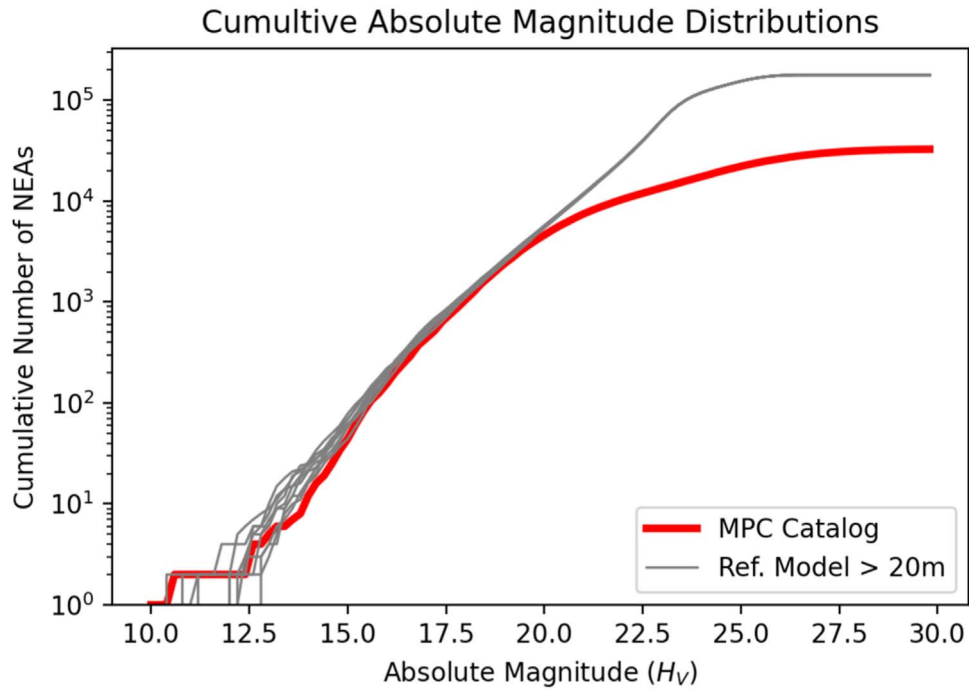
Cumulative Absolute Magnitude Distributions

Figure 5. The absolute magnitude distribution of 10 instances of the NEOS reference model for NEAs (solid gray lines) and the known population from the MPC catalog (solid red line) as of 2023 April.

Table 2
The Parameters of the KOM Used to Determine Which NEAs in the Model Should Be Considered Already Discovered at the Start of the NEOS Mission

| Years | Limiting Magnitude (*V* mag) | Field of Regard | | Chance of Discovery | Time Period |
		Longitude (deg)	Latitude (deg)		
1930–1949	14.0	30	15	50%	Historic period I
1950–1954	16.0	40	20	10%	Historic period II
1955–1959				0%	Historic period II
1960–1969	15.5	25	20	10%	Historic period III
1970–1979	16.0	30	25	25%	Historic period IV
1980–1989	17.1	30	20	30%	Palomar dominance
1990–1997	19.5	30	25	10%	Spacewatch dominance
1998–2001	19.5	40	30	85%	LINEAR start-up
2002–2004	20.0	45	30	90%	LINEAR dominance
2005–2010	20.6	45	30	75%	CSS dominance
2011–2013	21.1	45	30	75%	CSS dominance and PS start-up
2014–	21.5	45	30	90%	PS and CSS joint phase

MPC catalog as of the end of 2023 March. All of the results described in this work are based on running at least 10 instances of the NEA reference model through our modeling in a Monte Carlo approach.

4. NSS Known Object Model

In order to understand the progress of the NEOS mission toward the George E. Brown, Jr. goal, it is necessary to understand which of the synthetic objects in the reference model represent the objects that have already been found and cataloged by the MPC. The NSS uses a simple model to mimic the performance of the historical surveys over the last few decades. The model starts in 1970 and runs forward, tracking which objects in the reference model would be detected and when. For our analysis purposes, we assume that all discovery ends at the date of analysis, in this case the end of 2022, in order to understand a worst-case scenario. We can also extend

the model to predict which discoveries would be made up to the 2027 NEOS launch date for a best-estimate analysis as well.

The NSS model for determining what portion of the NEAs in the NEOS reference model are to be considered discovered at the start of the NEOS mission, hereafter called the KOM, uses four parameters that change with time. The four parameters controlling the KOM are the limiting magnitude, the size of the field of regard in ecliptic longitude and latitude, and the chance of discovery if the object is found to be inside the field of regard and brighter than the limiting magnitude. The model uses time steps of 30 days and computes the ecliptic position of each object in an instance of the reference model for each time step. The brightness of each object, V, is calculated using $V = H_V + 5\log(\Delta * r) - 2.5\log(F(G, \alpha))$, where Δ is the observer-to-object distance, r is the heliocentric distance of the object, α is the phase angle of the object, and $F()$ and G are the phase function and phase coefficient defined in Bowell et al.

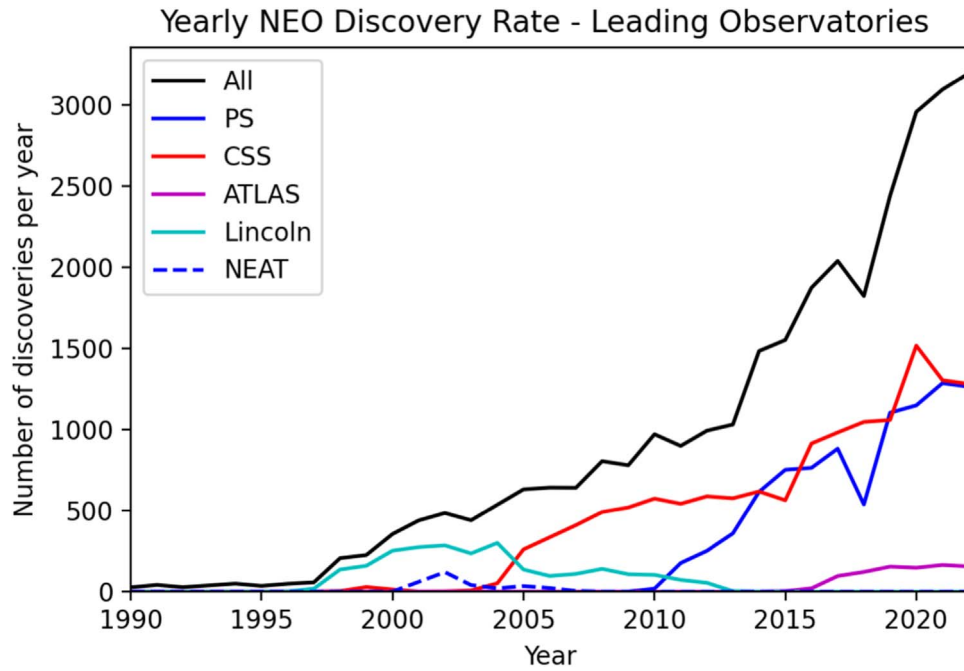## Yearly NEO Discovery Rate - Leading Observatories

Figure 6. The total discovery rate of NEAs per year is shown by a solid black line, with the yearly discovery rate of NEAs shown in different colored lines: PS (MPC sites F51 and 52) in solid blue and CSS (MPC sites 703 and G96) in solid red.

(1989). The field of regard is centered on the opposition point as seen from the Earth and on the ecliptic plane and has a half-width and half-height as shown in Table 2 (third and fourth columns, respectively). If the object is found to be in the field of regard and brighter than the limiting magnitude (see second column of Table 2) for the time step considered, the object has a chance of being considered discovered equal to that given in the fifth column in Table 2.

The values given in Table 2 are derived through a combination of methods. The first step is data analysis of the MPC catalog (downloaded on 2023 June 30) to determine which observatories dominate the various time periods over the last century (see Figure 6). By the end of the 1970s, only 80 NEAs were known, having been discovered by 22 different observatories, of which Palomar was the only site with more than a dozen discoveries (van Houten et al. 1970, 1984). The next decade, from 1980 to 1989, saw a doubling of the number of known NEAs to 185, with 10 additional telescope recording discoveries. Palomar, MPC site 675, dominated with 67 discoveries in this decade, with no other site achieving double-digit NEA discoveries. Over the next 6 yr, Palomar continued its work with ∼10 new discoveries per year, but this time period saw the rise of the Spacewatch survey at Kitt Peak, MPC site 691, which discovered 134 new NEAs over this time period (Gehrels & Jedicke 1996). Spacewatch was quickly superseded by the dawn of the Lincoln Near-Earth Asteroid Research (LINEAR; Stokes et al. 2000; Stuart 2001) program, MPC site 704, in 1997. LINEAR was the first observatory to reach more than 100 discoveries in the following year. LINEAR continued dominating the discovery of NEAs for 7 yr, discovering an average of 234 NEAs per year, until being superseded as the leading NEA discovery site by the CSS, MPC sites 703 and G96, in 2005 (Larson 2007; Zavodny et al. 2008; Granvik et al. 2018). CSS held the position as the leading yearly NEA discoverer for almost a decade, discovering an average of 477 new NEAs each year over this period. The next

major change in the search for NEAs came in 2011, with the introduction of the first of the PS telescopes (Denneau et al. 2013; Chambers et al. 2016), MPC site F51. By 2013, the field, led by the CSS and PS, had increased the number of discoveries to more than a thousand NEAs per year, of which more than 90% were discovered by those two dominating surveys. By the following year, the PS had matched the CSS in NEA discoveries per year at 616 new NEAs for PS and 618 new NEAs for CSS that year. In 2016, the CSS improved the equipment at their MPC site G96, more than doubling the discoveries per year at that site. This was followed just 2 yr later in 2018 by the introduction of the second telescope, MPC site F52, by PS, which gave this project a modest boost of ∼40% new discoveries per year.

For each of these time periods, we use the discovery observations in the MPC catalog from the known population of asteroids in the inner solar system (excluding any objects discovered past the orbit of Jupiter) to determine a starting point for each of the four parameters (see Figure 7 for an example of the magnitude parameter). Once the starting point has been determined, the KOM is run for a grid of values around these starting values, comparing the number of objects in the MPC catalog with the number of objects identified by the KOM as known for each time period and the absolute magnitudes of less than 17.75 mag, and less than each magnitude from 19 to, and including, 23 (the set $[< = 17.75, < = 19, < = 20, < = 21, < = 22, < = 23]$). The grid steps start at 0.5 mag for the limiting magnitude, with five degree steps for each field of regard parameter and 5% for the chance of discovery parameter. If none of the grid points yield an average of less than 10% difference for each magnitude limit at the end of the each time period, the grid points are halved, and the KOM is run for each of the new grid points. The resulting model parameter value represents the average value for that time period. We caution that the KOM is a simple first-order model that uses average values over the
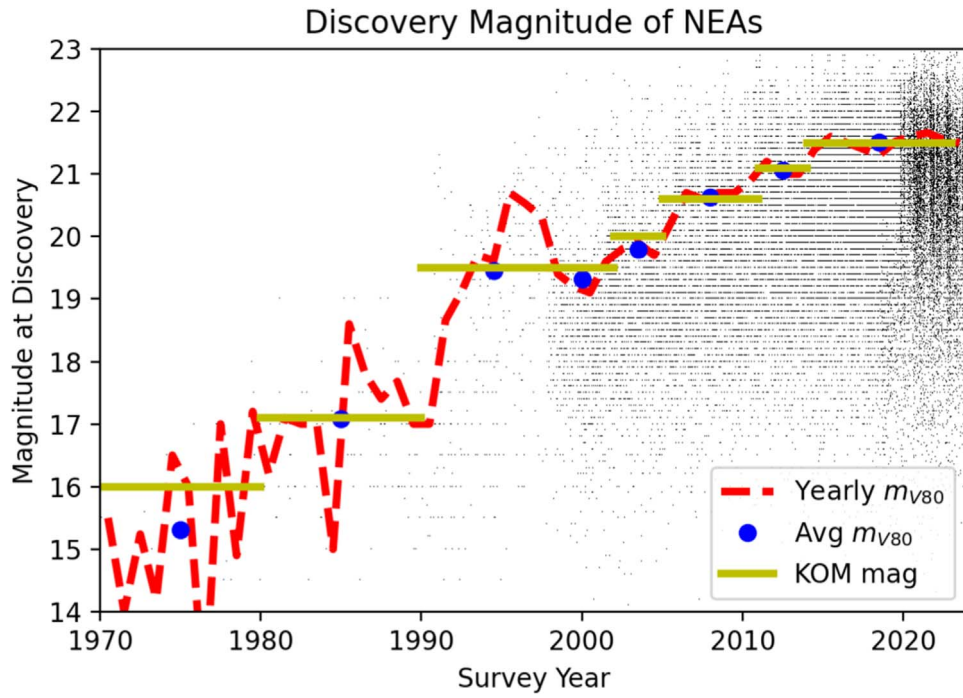
Figure 7. The discovery epoch magnitude reported to the MPC for each NEA cataloged from 1970 to 2023. The yearly 80th percentile value of the discovery magnitude, $m_V 80$, is given as a red dashed line, with the blue dots representing the average value of the $m_V 80$ for each time period given in Table 2. The yellow lines represent the value of the magnitude used in the KOM from Table 2.
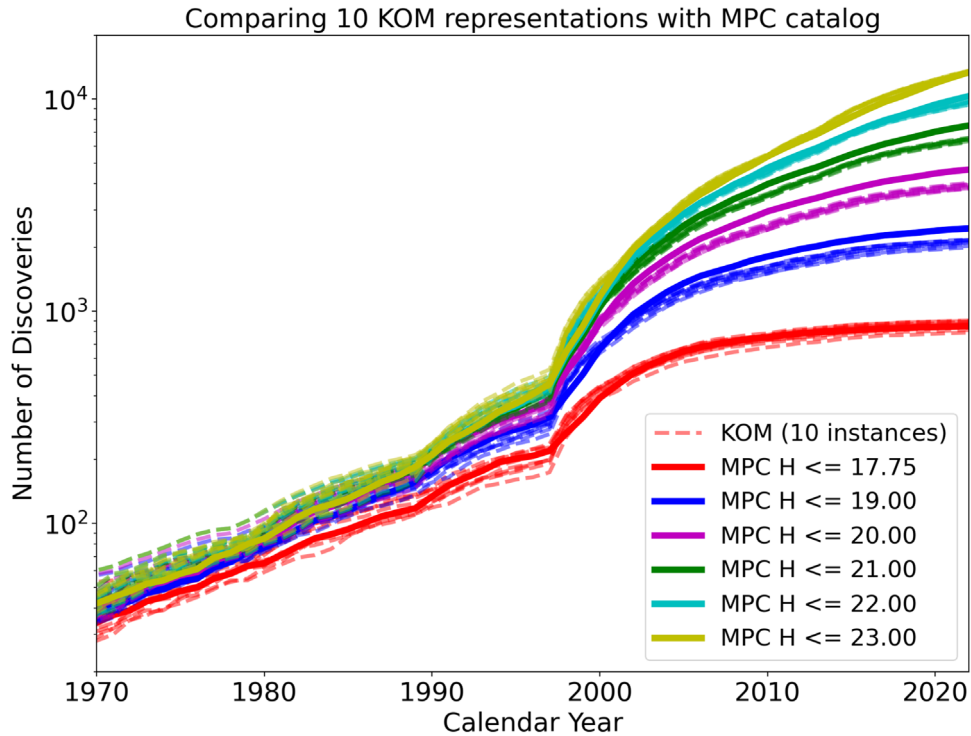

Figure 8. The comparison of the KOM using the NSS reference model with the known NEA population from the MPC at a range of absolute magnitude limits. The 10 random realizations of the NEA reference model were generated with a minimum effective diameter of 40 m.

stated time periods. Additional parameters, such as rate of motion cuts or different latitude limits for each hemisphere, are not considered, as initial tests show that this added granularity does not significantly improve the model results.

Figure 8 shows the discoveries of NEAs with H_V limits ranging from 17.75 (the traditional proxy of the 1 km objects)

to 23 (the proxy of 140 m objects) mag from 1980 to 2022 from both the MPC catalog and the KOM. The most prominent feature is the sharp increase in discoveries of NEAs in 1999, coinciding with the emergence of the LINEAR survey run by Lincoln Labs in New Mexico (Stokes et al. 2000). Another slight increase happens in the mid-2000s with the introduction

Table 3
Comparing the Average Number of Objects Found Using 10 Instances of the Reference Model with the Number of Known Objects at the End of Each Time Period in Table 2

Model Year	$H_V < 17.75$ mag			$H_V < 22$ mag			$H_V < 23$ mag		
	MPC	Model	Diff (%)	MPC	Model	Diff (%)	MPC	Model	Diff (%)
1949	16	15 ± 5	$+7.3 \pm 33.4$	19	17 ± 6	$+17.5 \pm 35.3$	19	20 ± 6	$+17.5 \pm 35.3$
1959	23	25 ± 7	$+9.1 \pm 28.3$	29	30 ± 7	$+3.8 \pm 25.4$	29	30 ± 7	$+4.8 \pm 24.8$
1969	33	32 ± 8	-2.7 ± 25.6	40	40 ± 9	$+0.8 \pm 21.4$	40	41 ± 8	$+2.5 \pm 19.8$
1979	63	63 ± 6	$+0.6 \pm 10.2$	80	84 ± 8	$+4.5 \pm 10.1$	80	85 ± 8	$+6.4 \pm 9.6$
1989	118	123 ± 10	$+4.4 \pm 8.7$	185	187 ± 13	$+1.1 \pm 7.3$	185	191 ± 14	$+3.4 \pm 7.3$
1997	220	210 ± 19	-4.5 ± 8.7	440	443 ± 25	$+0.6 \pm 5.7$	455	471 ± 31	$+3.5 \pm 6.6$
2001	447	464 ± 20	$+3.7 \pm 4.5$	1465	1442 ± 29	-1.5 ± 2.0	1556	1595 ± 33	$+2.5 \pm 2.1$
2004	603	598 ± 27	-0.8 ± 4.5	2504	2423 ± 55	-3.2 ± 2.2	2704	2758 ± 60	$+2.0 \pm 2.2$
2010	753	744 ± 32	-1.2 ± 4.3	4742	4482 ± 60	-5.5 ± 1.3	5372	5419 ± 63	$+0.9 \pm 1.2$
2013	798	787 ± 37	-1.4 ± 4.6	5909	5701 ± 68	-3.5 ± 1.1	6876	7130 ± 73	$+3.7 \pm 1.1$
2022	852	860 ± 36	$+1.0 \pm 4.2$	10334	9600 ± 120	-7.1 ± 1.2	13378	13458 ± 111	$+0.6 \pm 0.8$

of the CSS (Larson 2007), operated by the University of Arizona, and then again in the early 2010s by the introduction of the PS project, operated by the University of Hawaii (Denneau et al. 2013; Chambers et al. 2016).

Applying this model to an instance of the reference model, one can then compare the objects that are considered discovered in the reference model to the known population from the MPC catalog. Figure 8 shows the number of discoveries of NEAs for different limits of absolute magnitude, H_V, from 17.75 to 23 mag, which approximately spans the range from 1 km to 140 m. The number of discoveries reported to the MPC is given by the solid lines, while 10 instances of the NEA reference model (using a minimum diameter of 40 m) are plotted as dashed lines. Note that a model going down to 40 m is needed to evaluate the discovery rate down to the 140 m proxy of $H_V \sim 23$ mag, since an object with an effective diameter of 40 m and albedo of 0.5 would have an absolute magnitude of $H_V \sim 23.4$ mag. The KOM follows the major trends of the known population at all absolute magnitude cuts modeled. The final number of KOM objects with $H_V \leqslant 17.75$ mag identified as found at the end of 2022 was an average of 4.7% more than the number of objects with $H_V < 17.75$ mag in the MPC catalog of known objects. A total of 10 random realizations of the NEA reference model were created and processed through the KOM to assess the uncertainty (see Table 3). For the next three absolute magnitude limits of $H_V \leqslant 19$, 20, and 21 mag, the KOM underestimates the number of discovered objects by 12.1%, 13.1%, and 8.3%, respectively. For the $H_V < 22$ mag set, the KOM is in excellent agreement with the corresponding set from the MPC catalog, only overestimating the number of known objects by 1.7%. The difference grows again for $H_V \leqslant 23$ mag, where the KOM overestimates the number of known objects by 12.0%, on average, over the 10 randomly generated realizations of the NEA reference model.

The differences between the sample of synthetic objects identified by the KOM as known at the end of 2022 and those existing in the MPC catalog as seen in Table 3 are not surprising. Not only is the KOM a simplistic model, but the reference model makes a number of assumptions at smaller sizes due to the lack of information at sizes below 140 m. Specialty surveys, such as those conducted at low ecliptic solar elongation and NEOWISE (Mainzer et al. 2011b, 2012), account for about ∼10% of the discovered objects. These surveys generally have shallower limiting magnitudes or cover less area than the dominant opposition surveys. Since the KOM does not model these surveys, it is expected that it falls short in identifying objects in the NEA population, especially for $H_V \sim 18.5$–20.5 mag, which is the absolute magnitude range over which most of the specialty surveys have found objects that are not observable by the opposition surveys. For example, NEOWISE had discovered 393 NEAs by the end of 2022. Of these, 170 have $H_V \leqslant 20$ mag, which alone accounts for almost a quarter of the average difference of 730 objects when the KOM applied to 10 instances of the reference models is compared to the MPC catalog. For the $H_V \leqslant 21$ mag range, NEOWISE has discovered 274 NEAs, which accounts for ∼30% of the difference between the KOM and the MPC catalog. On the flip side, at $H_V \leqslant 22$ mag, the 328 NEA discoveries by NEOWISE would represent an increase of ∼3% in the difference between the model and catalog. To put these numbers in better perspective, we can examine the sample of $H_V \leqslant 23$ mag, the new proxy for 140 m NEAs. At this size range, Mainzer et al. (2011b, 2012) estimated that the uncertainty in our models is ±3000 for NEAs larger than 100 m. According to Harris & Chodas (2021), the completeness level at $H_V \leqslant 23$ mag is ∼30%, which means that our model assumptions introduce an error of ±1000 NEAs, which is significantly higher than the influence of surveys like NEOWISE not being included in the KOM.

The difference between the KOM and the known catalog of NEAs described above may also be partially driven by the assumptions used to generate the NEA reference model. The overabundance of objects found in the KOM for NEA with H_V is consistent with our reference model having an overabundance of objects with $H_V \sim 23$ mag. Mainzer et al. (2011b, 2012) estimated that there are $20,500 \pm 3000$ NEAs larger than 100 m. The NASA NEO Science Definition Report (SDT; Stokes et al. 2017) increased this to ∼25,000 NEOs larger than 140 m while acknowledging that this new estimate was larger than the previous result. This was attributed to using a single size–frequency distribution slope in the range $70 \text{ m} < D < 1.5 \text{ km}$, but they believed that the differences reflect the uncertainties that exist in the current size–frequency estimates. Thus, by selecting a reference model with 25,000 NEAs larger than 140 m in line with the SDT (Mainzer et al. 2023), the difference between the KOM and the MPC catalog of 1602 objects represents only ∼35% of this uncertainty, which is on the same order as the completeness for $H \leqslant 23$ mag derived by Harris & Chodas (2021). Heinze et al. (2021) also
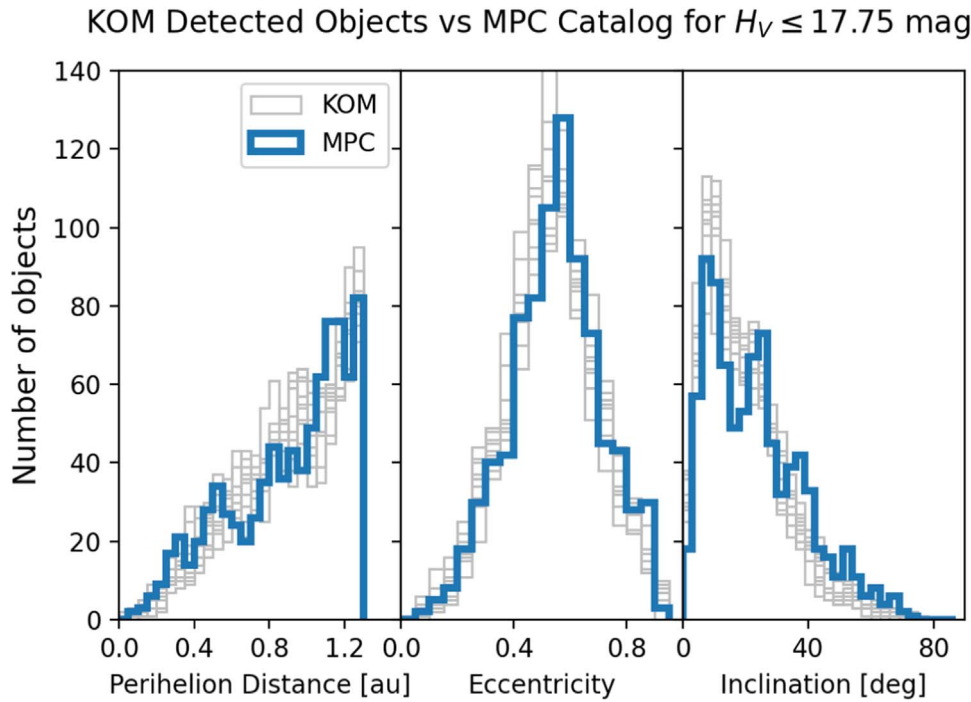
Figure 9. The comparison of the KOM using the reference model with the known NEA population from the MPC for objects with $H_V \leqslant 17.75$ mag (the proxy for objects larger than ~ 1 km). The orbital elements of perihelion distance, eccentricity, and inclination are shown from left to right. The KOM applied to 10 random realizations of the NEA reference model is shown in gray, while the MPC distribution is shown in blue.

found that NEOs smaller than $H_V \sim 22.5$ mag are more common than expected using extrapolation of the size–frequency distribution at larger sizes. In conclusion, it is clear that our understanding of the size–frequency distributions smaller than $H_V \sim 22.5$ mag is not well understood, which is exactly the range where a survey like NEOS will be most efficient. It is thus not unreasonable to conclude that the differences between the model presented in this paper and the MPC catalog at $H \leqslant 23$ mag are primarily driven by an overabundance of these objects in our reference model.

Some other reasons for the differences between the number of objects detected by the KOM and the number of objects cataloged by MPC have been considered. As seen in Figure 2, the fractions based on the known population remain relatively stable over the absolute magnitude range covered in this analysis, and the relative fraction of objects as a function of diameter is kept constant during the construction of the NEA reference model. However, the distribution among the subpopulations shown in Figure 2 is based on the raw observed data and may contain observational biases that are not well understood and therefore not incorporated into the KOM. Other similar assumptions, such as the albedo distribution being the same across all diameter bins for each subpopulation, may also not hold, but these assumptions remain the best knowledge we currently have about the NEA population. Furthermore, the reference model makes a number of assumptions at smaller sizes due to the lack of information at sizes below 140 m. It is possible that a break in the size–frequency distribution exists somewhere around ~ 100 m, although the location and magnitude of this break remain uncertain (Harris & D'Abramo 2015; Granvik et al. 2018; Harris & Chodas 2021). Such a break would change the relative number of NEAs in the different absolute magnitude limit samples, with objects of 100 m having absolute magnitudes of $H_V \sim 21$–25 mag. It is in

part due to the uncertainty of the validity of these assumptions that the future generation of surveys, such as NEOS, are of such importance. These future surveys are key in testing our current assumptions and knowledge about the NEA population and will provide new and improved NEA reference models that will help us better understand the danger the NEA population poses.

While the KOM provides a reasonable estimate of the discovery rates of the MPC catalog over the last few decades for a range of absolute magnitude bins, it is also important to make sure that the model is identifying all types of objects regardless of orbital elements and physical properties. Figures 9 and 10 compare the orbital elements of the synthetic population the KOM identified as found compared to the orbital elements of the known objects in the MPC catalog for two absolute magnitude limits. Both figures show agreement between the distributions in semimajor axis, eccentricity, and inclination. One noticeable difference in the $H \leqslant 23$ mag sample is a slight underestimation of found Amor objects in the KOM, which indicates that the Amor population may be slightly underestimated in the NEOS reference model.

We can also look at the observational biases that exist in a pure opposition survey, which is what the KOM represents. The lack of any Atira asteroids detected in the KOM is one of the clearest biases, but there are also interesting biases among the other subpopulations. When studying the fraction of objects detected as a function of H_V (see Figure 11), it is seen that for the larger objects, $H_V \sim 16$ mag, the Amor subpopulation is favored by almost 3% higher completeness over objects in the Apollo subpopulation. This difference increases to almost 10% higher completeness at $H_V \sim 21$ mag. At $H_V > 23$ mag, the difference in the chance of detection drops to close to zero between these two populations. For the Aten population, the observational biases are significant at larger sizes, with only
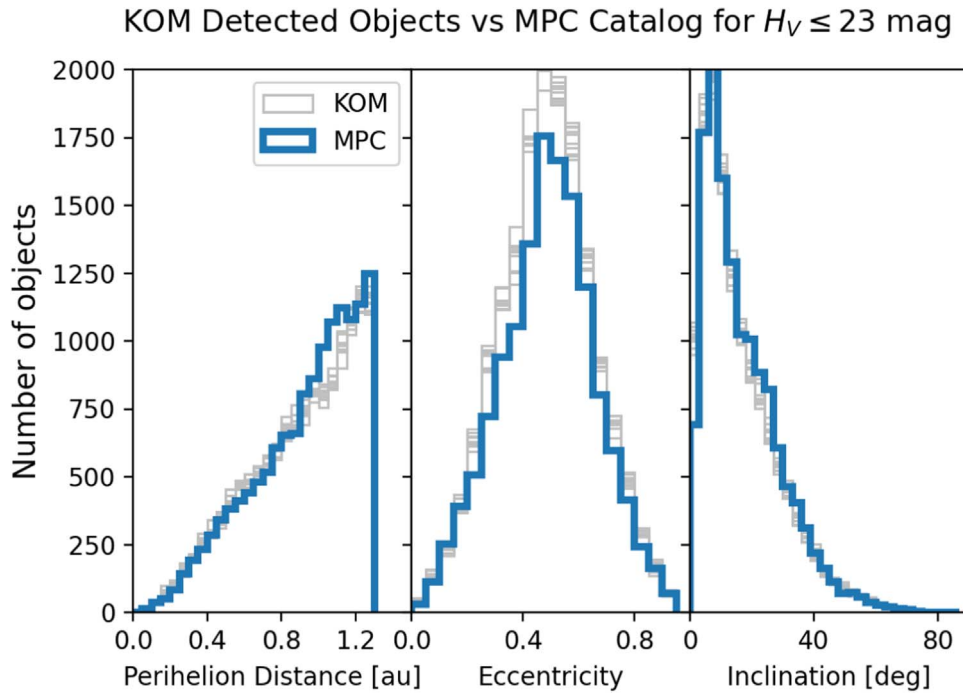
KOM Detected Objects vs MPC Catalog for $H_V \leq 23$ mag

Figure 10. The comparison of the KOM using the NEA reference model with the known NEA population from the MPC for objects with $H_V \leqslant 23$ mag (the proxy of objects larger than ∼140 m). The orbital elements of perihelion distance, eccentricity, and inclination are shown from left to right. The KOM applied to 10 random realizations of the NEA reference model is shown in gray, while the MPC distribution is shown in blue.
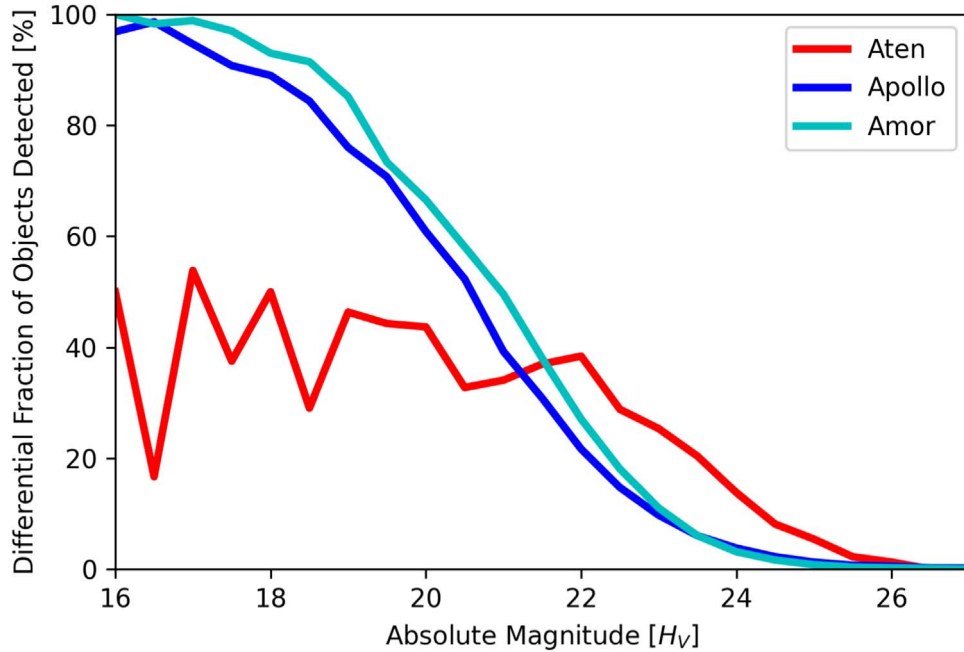
Figure 11. The fraction of objects observed by the KOM as a function of absolute magnitude H_V in bins of ±0.25 mag around the absolute magnitude. The Amor subpopulation is favored by almost 10% for $H_V < 23$ mag over the Apollo subpopulation. For objects with $H_V > 23$ mag, there is little difference in the biases of these two subpopulations. The Atens have significantly higher chances of being detected by the KOM for $H_V > 22$ mag.

∼40% of objects detected in the 18 mag $< H_V <$ 22 mag range. At fainter magnitudes, $H_V > 23$ mag, opposition surveys are more likely to detect Atens, relative to both Apollos and Amors. These biases are a combination of the observational geometry and the on-sky location where the survey is operating, primarily centered on opposition.

Assuming that the KOM is a reasonable estimate of the known objects currently cataloged by the MPC, we examine the completeness of the current catalog. The cumulative completeness as a result of the KOM for objects with diameters larger than a specific diameter limit is shown in Figure 12. For the larger objects with $D \geqslant 1$ km, the KOM finds a completeness of 87%, which is slightly below the 90% completeness found by Mainzer et al. (2011a) and Granvik et al. (2018). This is mainly due to the lack of low solar angle surveys in the KOM, with NEOWISE alone having contributed
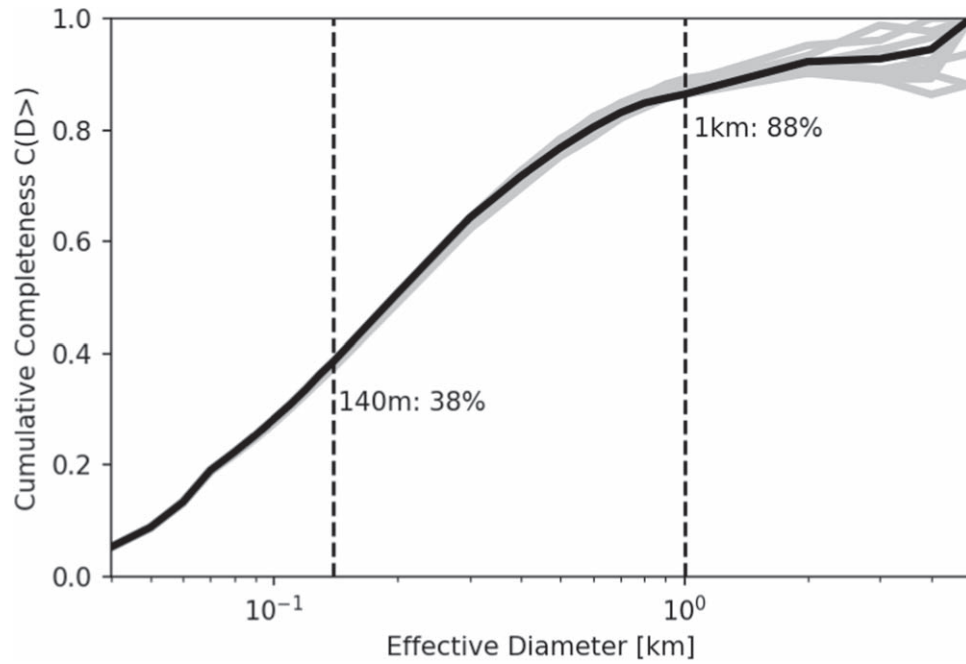
Figure 12. Cumulative completeness of the diameter, $C(D>)$, at the end of 2022 as a result of the KOM computed for 10 random realizations of the NEA reference model with the minimum size set to 40 m. The average cumulative completeness is shown as the solid line, showing that the KOM estimates an average completeness of 88% for NEAs larger than 1 km and 38% for NEAs larger than 140 m. The discrepancy between our completeness estimate at 1 km and the estimates of 90+% completeness from Mainzer et al. (2011a) and Granvik et al. (2018) are due to the fact that the KOM does not include specialty surveys (such as the low solar elongation surveys, NEOWISE, etc.). NEOWISE has, for example, contributed at least 55 NEA discoveries with diameters larger than 1 km, which would account for ∼6% of completeness for this size range.
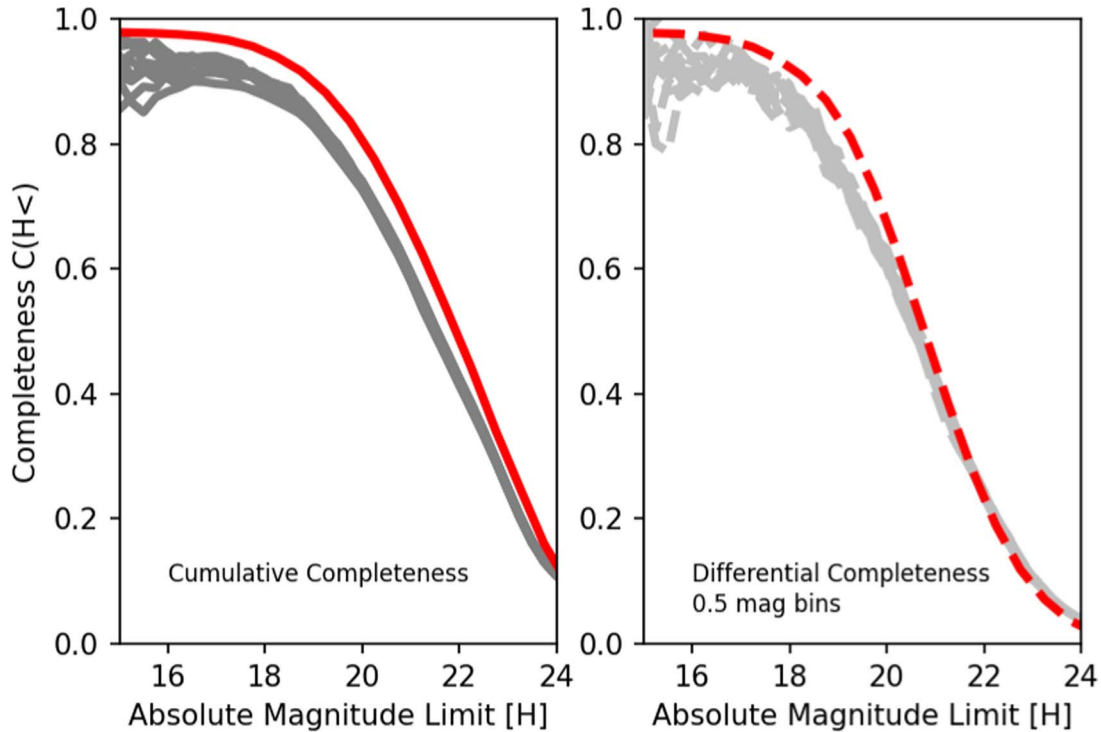
Figure 13. Cumulative and differential completeness of the absolute magnitude, $C(H_V <)$, at the end of 2022 as a result of the KOM for 10 instances of the reference model with the minimum size set to 40 m. The differential completeness is shown as the light gray solid lines, while cumulative completeness is shown as the dark gray solid lines. The cumulative and differential completenesses as a function of absolute magnitude as derived by Harris & Chodas (2021) are shown as the solid and dashed red lines, respectively. The missing completeness in the KOM at $H_V < 20$ mag is due to the KOM not modeling the low solar elongation surveys and NEOWISE.

351 new discoveries not accounted for in the KOM. Of these, at least 55 are larger than 1 km (Nugent et al. 2015, 2016; Masiero et al. 2017, 2020, 2021). On average, our 10 random realizations of the NEA reference model have 997 ± 39 NEAs larger than 1 km, with the KOM yielding a completeness of, on average, $88\% \pm 1\%$ for this size regime. Thus, the additional
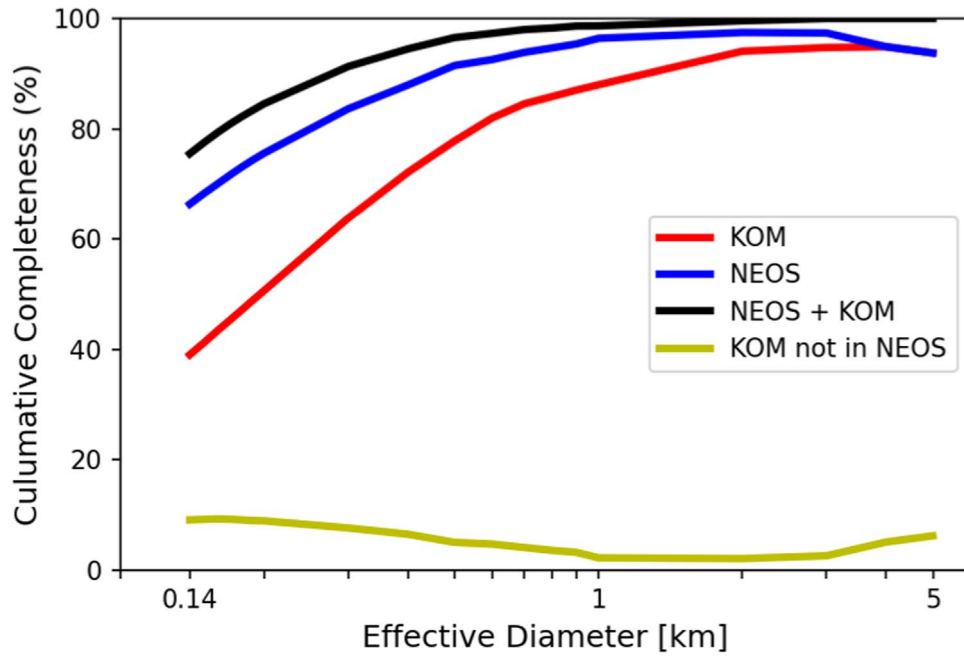
Figure 14. The cumulative completeness of the effective diameter for NEAs in the reference model for the KOM (red solid line), the NEOS mission (blue solid line), and the combined result of the KOM and the NEOS mission (black solid line). Also shown is the fraction of objects seen by KOM that NEOS is not likely to detect in its 5 yr nominal mission (yellow solid line).
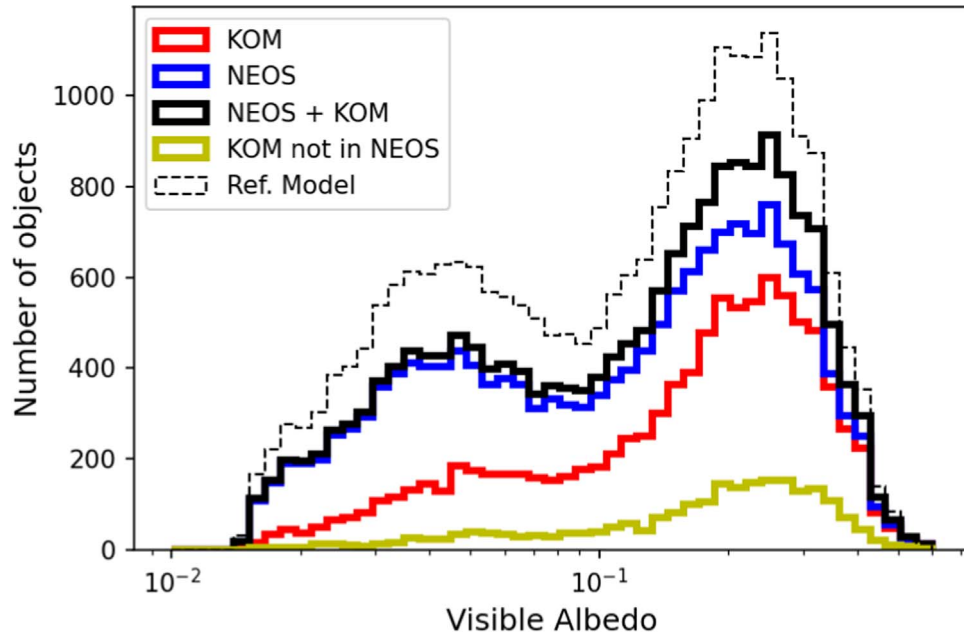

Figure 15. The visible albedo distribution of the objects that are larger than 140 m from an instance of the reference model identified by the KOM (red histogram) as currently cataloged. The objects identified as cataloged by NEOS are given as a blue histogram, with the combined set of objects cataloged by both KOM and NEOS shown as a black histogram. The NEAs larger than 140 m that are identified as cataloged by the KOM and not seen by the NEOS in a nominal 5 yr survey are shown as the yellow histogram.

discoveries provided by NEOWISE represent a significant portion of the difference between the completeness derived by the KOM and that found by Mainzer et al. (2011a) and Granvik et al. (2018).

For the objects larger than 140 m, the KOM returns a completeness of $\sim 38.3\% \pm 0.3\%$ at the end of 2022 when applied to 10 instances of the reference model. This is consistent with the completeness derived by Harris & Chodas (2021), which found 44% completeness for $H_V < 22.25$ mag, 34% completeness for $H_V < 22.75$ mag, and 25% completeness

for $H_V < 23.25$ mag. Harris & Chodas (2021) relied mainly on optical observations and thus derived completeness estimates, both cumulative and differential, as functions of absolute magnitude. Figure 13 shows their results compared to the completeness modeled by the KOM across different absolute magnitude limits. It shows that KOM underestimates the completeness down to $H_V \sim 21$ mag, which is consistent with the low solar elongation surveys, such as NEOWISE, not being modeled by KOM. At $H_V \leqslant 23$ mag, our proxy for an effective diameter of 140 m, the KOM, and the Harris & Chodas (2021)
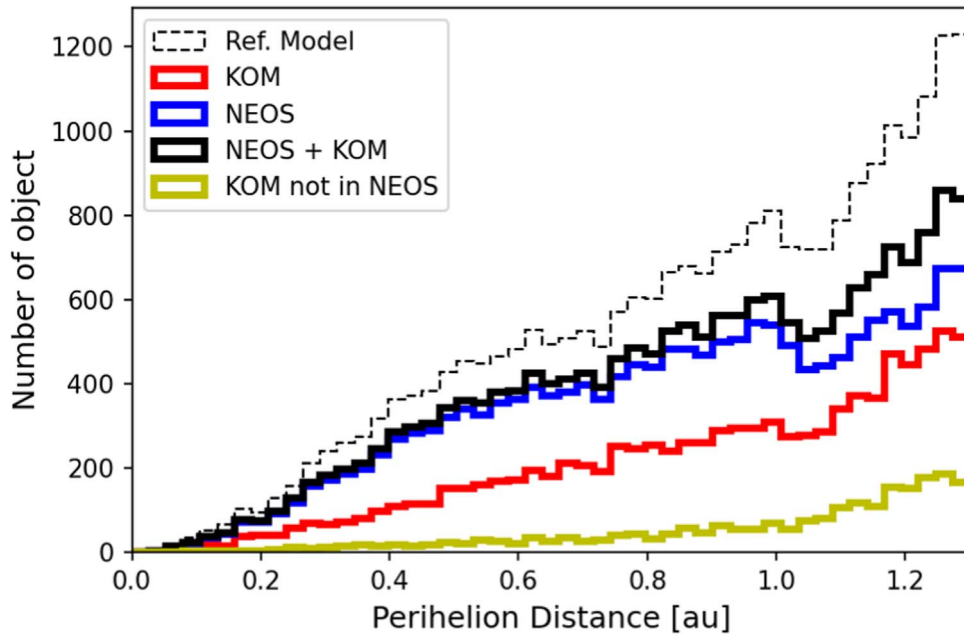
Figure 16. The distribution of perihelion distance for the objects cataloged by KOM up until the end of 2022 (red histogram), the NEOS 5 yr nominal mission (blue histogram), and the two combined (black solid histogram). The distribution of objects identified as cataloged by KOM that are not observed by NEOS is shown as a yellow histogram. This shows that the majority, ∼59%, of known objects missed by the NEOS are Amors, where the current surveys are fairly efficient due to the favorable geometry.
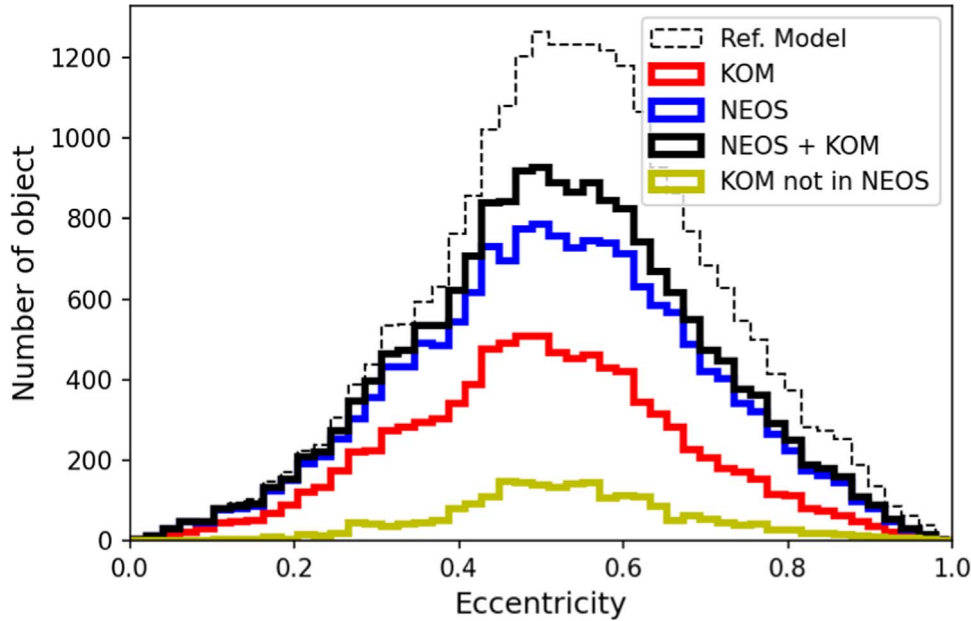

Figure 17. The eccentricity distribution of the objects cataloged by KOM up until the end of 2022 (red histogram), NEOS 5 yr nominal mission (blue histogram), and the two combined (black solid histogram). The distribution of objects identified as cataloged by KOM that are not observed by NEOS are shown as a yellow histogram. As expected, NEOS is very efficient at detecting and tracking low-eccentricity objects, similar to the current surveys.

results are in reasonable agreement. Note that the flattening of the cumulative distribution at $H_V > 24$ mag is due to the limit in H_V imposed by limiting the reference model used to 40 m or larger.

5. KOM Objects and NEOS

One of the questions faced by the NEOS mission is understanding which synthetic objects identified as known by the KOM would and would not be seen by the observatory over its nominal mission. Objects that are both observed in the optical by ground-based surveys (such as those modeled as detected by KOM) and detected in the thermal by NEOS during its nominal 5 yr survey are of particular interest, as both their diameters and albedos can be determined. When applying the NSS with a nominal 5 yr survey planning model to the reference model for NEAs described in Mainzer et al. (2023), we find that for NEAs larger than 140 m, ∼77% of the ∼9750 objects that the KOM identified as currently known will also be detected and tracked by NEOS during its nominal survey. Thus, almost one-third of the NEAs larger than 140 m will have both optical and thermal observations collected at the end of the
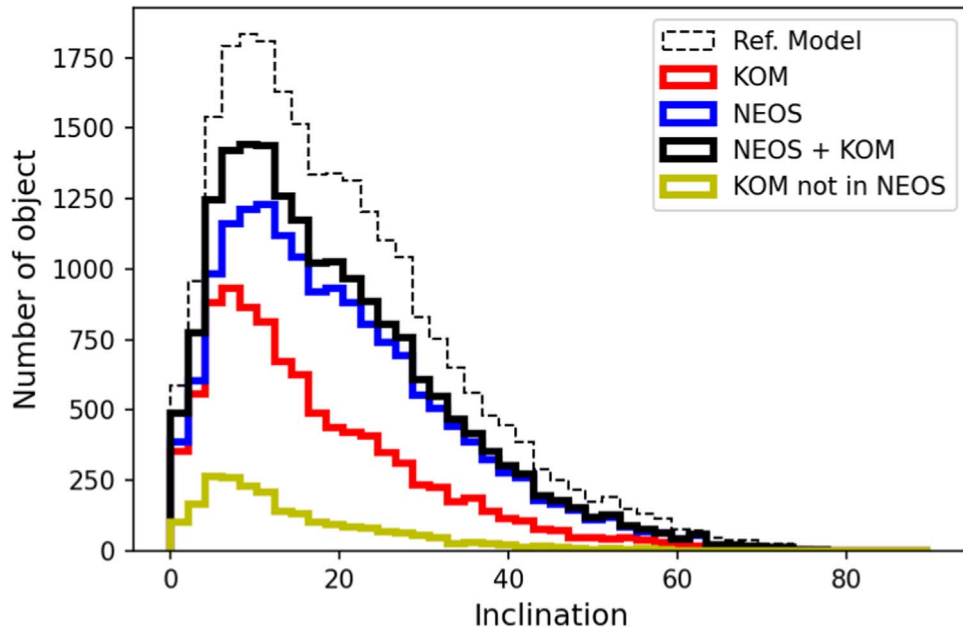
Figure 18. The inclination distribution of the objects cataloged by KOM up until the end of 2022 (red histogram), NEOS (blue histogram), and the two combined (black solid histogram). The distribution of objects identified as cataloged by KOM that are not observed by NEOS are shown as a yellow histogram. NEOS is found to be slightly more efficient at detecting and tracking the higher-inclination NEOS ($i > \sim 15°$) than the current surveys.

NEOS 5 yr mission, providing diameter and albedo for an order of magnitude more NEAs with diameters larger than 140 m than are available today (Mainzer et al. 2019; Masiero et al. 2021). Of course, there will also be numerous smaller NEAs with both optical and thermal measurements that will also significantly contribute to the understanding of the NEA populations' physical properties.

Another set of objects of interest is the objects that are already known that will not be detected by NEOS during its nominal mission. While neither diameter nor albedo can be determined for these objects, knowledge of their orbital parameters means that they will remain part of the catalog of known objects, contributing to the final PHA and NEA completeness reached at the end of the NEOS survey. The remaining objects, those that were identified as already known by the KOM but are not likely to be detected by the NEOS, contribute 8%–9% to the total completeness of the catalog at the end of the NEOS nominal mission. Figure 14 shows that the KOM-estimated survey completeness for NEAs larger than 140 m was ∼38% as of the end of 2022. Also shown is the completeness of a single random realization of the reference model for NEAs larger than 140 m, simulating the performance of the NEOS's nominal 5 yr survey. Without any prior knowledge from ground-based surveys, the cumulative completeness from NEOS's 5 yr nominal survey is ∼66% for this size regime. When combining the KOM and NEOS results, the final catalog of known objects would be ∼76% complete. For the PHAs, the completeness is predicted to be 82% (Mainzer et al. 2023) at the end of the NEOS 5 yr mission. As expected, NEOS and the KOM combine to find nearly all NEAs larger than 1 km.

When looking at the albedo distributions, the observational biases toward the higher-albedo NEAs are clearly seen in the objects identified as cataloged by the KOM (see Figure 15). This feature was pointed out in Mainzer et al. (2011b, 2012). As with the NEOWISE results, NEOS is almost free of biases in albedo and detects objects of all albedos nearly equally well.

Examining the orbital elements of the objects identified by the KOM and NEOS (see Figures 16–18) shows that ground-based surveys, according to the KOM, are slightly more efficient at detecting Amors (∼42% completeness at the end of 2022) compared to the Apollos (∼38% completeness) and Atens (∼35% completeness) for objects larger than 140 m. For the same size regime, NEOS is more efficient at detecting Atiras, Atens, and Apollos than Amors, with NEOS detecting ∼88% of Atiras, ∼95% of Atens, ∼71% of Apollos, and ∼57% of Amors during its 5 yr mission. The synergy between the currently known object catalog and the objects detected and tracked by NEOS becomes apparent when looking at the ∼9% of NEAs in the reference model larger than 140 m that are identified as cataloged and not seen by NEOS (see Figure 16). A majority, ∼59%, of this set of objects are Amors, followed by ∼40% Apollos and less than 1% Atens.

When looking at the eccentricity distributions (see Figure 17), the combination of the currently cataloged objects and the objects discovered by NEOS account for almost all objects with eccentricity less than 0.4. The objects with higher eccentricity spend more time further away from the Earth's orbit and need to be closer to the perihelion point in their orbits to be detected and tracked. This can be remedied by extending the NEOS survey duration, giving these objects more time to approach their perihelia when passing through the NEOS field of regard. The inclination distributions (see Figure 18) show similar trends, with nearly all low-inclination objects being cataloged by a combination of the KOM and the NEOS. A vast majority of the objects that are not cataloged have inclinations of 15° or more.

6. Conclusions

In this paper, we have shown that, using a simple model called the known object model (KOM), we can provide a reasonable estimate of which NEAs in the reference population model created for the NEO Surveyor (NEOS) mission are currently known. These objects represent the combined efforts

of mainly ground-based surveys such as LINEAR (Stokes et al. 2000, 2002), the Catalina Sky Survey (Larsen et al. 2007), and the Pan-STARRS project (Wainscoat et al. 2010; Chambers et al. 2016). The simple model approximately recreates the NEA discovery rate recorded by the MPC catalog over a wide range of absolute magnitudes, $H_V \sim 17$–23 mag.

When applying the KOM to a set of randomly generated realizations of the NEOS reference model, it is estimated that the catalog completeness of NEAs larger than 140 m at the end of 2022 stands at $\sim$38%, which is consistent with the results of Harris & Chodas (2021) when using $H_V < 23$ mag as a proxy for this population. It is further found that $\sim$77% of the objects larger than 140 m cataloged by the KOM are identified as also being detected by NEOS in a 5 yr nominal survey. The remaining set of objects larger than 140 m cataloged by the KOM and not detected by NEOS represents $\sim$9% of the total number of NEAs larger than 140 m in the NEOS reference model. These two sets of objects can be combined with the objects cataloged by NEOS to derive a modeled catalog completeness of $\sim$76% for NEAs larger than 140 m and $\sim$82% for PHAs larger than 140 m at the end of the NEOS 5 yr baseline mission (Mainzer et al. 2023).

Acknowledgments

ORCID iDs

Tommy Grav ⓘ https://orcid.org/0000-0002-3379-0534
Amy K. Mainzer ⓘ https://orcid.org/0000-0002-7578-3885
Joseph R. Masiero ⓘ https://orcid.org/0000-0003-2638-720X
Dar W. Dahlen ⓘ https://orcid.org/0000-0003-1876-9988
William F. Bottke ⓘ https://orcid.org/0000-0002-1804-7814
Frank J. Masci ⓘ https://orcid.org/0000-0002-8532-9395

References

Alvarez, L. W., Alvarez, W., Asaro, F., & Michel, H. V. 1980, Sci, 208, 1095
Astropy Collaboration, Price-Whelan, A. M., Lim, P. L., et al. 2022, ApJ, 935, 167
Bauer, J. M., Grav, T., Fernández, Y. R., et al. 2017, AJ, 154, 53
Bottke, W. F., Morbidelli, A., Jedicke, R., et al. 2002, Icar, 156, 399
Bowell, E., Hapke, B., Domingue, D., et al. 1989, in Asteroids II, ed. R. P. Binzel, T. Gehrels, & M. S. Matthews (Tucson, AZ: Univ. Arizona Press), 524
Chambers, K. C., Magnier, E. A., Metcalfe, N., et al. 2016, arXiv:1612.05560
Denneau, L., Jedicke, R., Grav, T., et al. 2013, PASP, 125, 357
Gehrels, T., & Jedicke, R. 1996, EM&P, 72, 233
Granvik, M., Morbidelli, A., Jedicke, R., et al. 2018, Icar, 312, 181
Grav, T., Mainzer, A. K., & Spahr, T. 2016, AJ, 151, 172
Harris, A. W., & Chodas, P. W. 2021, Icar, 365, 114452
Harris, A. W., & D'Abramo, G. 2015, Icar, 257, 302
Harris, C. R., Millman, K. J., van der Walt, S. J., et al. 2020, Natur, 585, 357
Heinze, A. N., Denneau, L., Tonry, J. L., et al. 2021, PSJ, 2, 12
Jones, R. L., Slater, C. T., Moeyens, J., et al. 2018, Icar, 303, 181
Kluyver, T., Ragan-Kelley, B., Pérez, F., et al. 2016, in Positioning and Power in Academic Publishing: Players, Agents and Agendas, ed. F. Loizides & B. Scmidt (Amsterdam: IOS Press), 87
Larsen, J. A., Roe, E. S., Albert, C. E., et al. 2007, AJ, 133, 1247
Larson, S. 2007, in IAU Symp. 236, Near Earth Objects, our Celestial Neighbors: Opportunity and Risk, ed. G. B. Valsecchi, D. Vokrouhlický, & A. Milani (Cambridge: Cambridge Univ. Press), 323
Mainzer, A., Bauer, J., Grav, T., et al. 2011a, ApJ, 731, 53
Mainzer, A., Grav, T., Bauer, J., et al. 2011b, ApJ, 743, 156
Mainzer, A., Grav, T., Bauer, J., et al. 2015, AJ, 149, 172
Mainzer, A., Grav, T., Masiero, J., et al. 2011c, ApJ, 736, 100
Mainzer, A., Grav, T., Masiero, J., et al. 2012, ApJ, 752, 110
Mainzer, A. K., Bauer, J. M., Cutri, R. M., et al. 2019, NEOWISE Diameters and Albedos V2.0, urn:nasa:pds:neowise_diameters_albedos::2.0. NASA Planetary Data System
Mainzer, A. K., Masiero, J. R., Bauer, J. M., et al. 2023, PSJ, 4, 224
Masiero, J. R., Dahlen, D. W., Mainzer, A. K., & Grav, T. 2023, PSJ, 4, 225
Masiero, J. R., Mainzer, A. K., Bauer, J. M., et al. 2020, PSJ, 1, 5
Masiero, J. R., Mainzer, A. K., Bauer, J. M., et al. 2021, PSJ, 2, 162
Masiero, J. R., Nugent, C., Mainzer, A. K., et al. 2017, AJ, 154, 168
Milani, A., Carpino, M., & Marzari, F. 1990, Icar, 88, 292
Morrison, D. 1992, Mercu, 21, 103
National Academies of Sciences, Engineering, and Medicine 2019, Finding Hazardous Asteroids Using Infrared and Visible Wavelength Telescopes (Washington, DC: The National Academies Press),
Nugent, C. R., Mainzer, A., Bauer, J., et al. 2016, AJ, 152, 63
Nugent, C. R., Mainzer, A., Masiero, J., et al. 2015, ApJ, 814, 117
Pravec, P., Harris, A. W., Kušnirák, P., Galád, A., & Hornoch, K. 2012, Icar, 221, 365
Scott, D. W. 1992, Multivariate Density Estimation (New York: Wiley)
Stokes, G. H., Barbee, B. W., Bottke, W. F., et al. 2017, Update to Determine the Feasibility of Enhancing the Search and Characterization of NEOs. Report of the Near-Earth Object Science Definition Team, NASA https://cneos.jpl.nasa.gov/doc/SDT_report_2017.html
Stokes, G. H., Evans, J. B., & Larson, S. M. 2002, in Asteroids III, ed. W. F. Bottke, Jr. et al. (Tucson, AZ: Univ. Arizona Press), 45
Stokes, G. H., Evans, J. B., Viggh, H. E. M., Shelly, F. C., & Pearce, E. C. 2000, Icar, 148, 21
Stokes, G. H., Yeomans, D. K., Bottke, W. F., et al. 2003, Study to Determine the Feasibility of Extending the Search for Near-Earth Objects to Smaller Limiting Diameters. Report of the Near-Earth Object Science Definition Team, NASA https://cneos.jpl.nasa.gov/doc/SDT_report_2003.html
Stuart, J. S. 2001, Sci, 294, 1691
Tedesco, E. F., Noah, P. V., Noah, M., & Price, S. D. 2002, AJ, 123, 1056
Tedesco, E. F., Veeder, G. J., Fowler, J. W., & Chillemi, J. R. 1992, The IRAS Minor Planet Survey, Tech. Rep. PL-TR-92-2049, Philliips Laboratory, Hanscom Air Force Base, MA https://irsa.ipac.caltech.edu/IRASdocs/surveys/PL-TR-92-2049.pdf
Usui, F., Kuroda, D., Müller, T. G., et al. 2011, PASJ, 63, 1117
van Houten, C. J., Herget, P., & Marsden, B. G. 1984, Icar, 59, 1
van Houten, C. J., van Houten-Groeneveld, I., Herget, P., & Gehrels, T. 1970, A&AS, 2, 339
Vereš, P., & Chesley, S. R. 2017, AJ, 154, 13
Virtanen, P., Gommers, R., Oliphant, T. E., et al. 2020, NatMe, 17, 261
Wainscoat, R. J., Jedicke, R., Denneau, L., et al. 2010, BAAS, 42, 1085
Wetherill, G. W. 1987, RSPTA, 323, 323
Wetherill, G. W. 1988, Icar, 76, 1
Wright, E. L., Mainzer, A., Masiero, J., Grav, T., & Bauer, J. 2016, AJ, 152, 79
Zavodny, M., Jedicke, R., Beshore, E. C., Bernardi, F., & Larson, S. 2008, Icar, 198, 284